Biosensors and Bioelectronics 61 (2014) 38–44

Contents lists available at ScienceDirect

Biosensors and Bioelectronics

journal homepage: www.elsevier.com/locate/bios

Highly sensitive and selective determination of bisphenol-A using peptide-modified gold electrode

Jiao Yang [a], Sung-Eun Kim [a], Misuk Cho [a], Ik-Keun Yoo [b], Woo-Seok Choe [a,*], Youngkwan Lee [a,*]

[a] School of Chemical Engineering, Sungkyunkwan University, Suwon 440-746, Republic of Korea
[b] School of Chemical Engineering and Bioengineering, University of Ulsan, Ulsan 680-749, Republic of Korea

ARTICLE INFO

Article history:
Received 20 December 2013
Received in revised form
3 April 2014
Accepted 3 April 2014
Available online 28 April 2014

Keywords:
Peptide
Bisphenol A
Self-assembled monolayer
Differential pulse voltammetry
Biosensor

ABSTRACT

Fast and accurate determination of bisphenol A (BPA) in varying matrices has become important in recent years. In this study, a cysteine-flanked heptapeptide sequence Cys-Lys-Ser-Leu-Glu-Asn-Ser-Tyr-Cys (CKSLENSYC), which is capable of recognizing BPA with high specificity, was isolated using a phage display technique. A novel electrochemical biosensor harnessing this affinity peptide as a BPA detection probe, was constructed and its performance was assessed. The formation of a self-assembled peptide monolayer on the gold electrode was confirmed by attenuated total reflection infrared spectroscopy (ATR-IR), cyclic voltammetry (CV) and electrochemical impedance spectroscopy (EIS). Following the exploration of the optimum sensing condition, differential pulse voltammetry (DPV) was used to determine the varying concentrations of BPA in the solution. The developed sensor conveyed excellent performance in view of sensing speed, sensitivity and selectivity by detecting BPA in less than 5 min with a broad dynamic detection range of 1–5000 nM of BPA, despite the presence of several interfering species, such as phenolic compounds and inorganic ions.

© 2014 Elsevier B.V. All rights reserved.

1. Introduction

Bisphenol A (BPA), an organic compound with two phenol functional groups, is widely used as an important monomer for the production of plastics, such as polycarbonates (PC) and epoxy resins. In addition, it is extensively used in adhesives and flame retardants (Podlipna and Cichna-Markl, 2007) as well as an antioxidant in plasticizers and a polymerization inhibitor for polyvinyl chloride (PVC). BPA is released into the environment primarily via wastewater during the manufacturing process or by leaching from commercial PC or epoxy resin products, including baby bottles, water bottles, eyeglass lenses, coatings on food package, and beverage cans (Zhang et al., 2011; Wu et al., 2012; Gao et al., 2012). Further, BPA has been implicated as an endocrine disruptor that is capable of mimicking natural hormones, thereby leading to negative health effects and increased cancer risk. In 2008, Lang's group reported that the accumulation of BPA in the human body was closely associated with heart diseases, diabetes and cancer. Furthermore, due to increasing public concerns over the impact of BPA exposure on infants and children, Canada and China declared BPA as a toxic substance and therefore banned the use of BPA in baby bottles in 2010 and 2011, respectively (Wu et al., 2012; Gao et al., 2012). Thus, it is of critical importance to develop a fast, simple and reliable method for trace level determination of BPA in various specimens.

Various analytical approaches harnessing high performance liquid chromatography (HPLC) (Lin et al., 2011a), liquid chromatography–mass spectrometry (LC–MS) (Yan et al., 2009), gas chromatography–mass spectrometry (GC–MS) (Martínez-Moral and Tena, 2011), enzyme-linked immunosorbent assay (ELISA) (Lu et al., 2012), molecular imprinting technique (Ren et al., 2012) and electrochemical method (Fan et al., 2012; Yin et al., 2011) have been applied to the measurement of BPA. Among them, the electrochemical method has a great potential for the environmental monitoring of BPA in view of its high sensitivity and fast response that is achievable in a simple and cost-efficient manner. To enable an electrochemical detection of BPA, various types of electrodes have been fabricated with the use of enzymes (Wu et al., 2012), antibodies (Piao et al., 2008), aptamers (Kang et al., 2011), carbon nanotubes (Gao et al., 2012), nanoparticles (Tu et al., 2009) and graphene (Fan et al., 2012). However, the insufficient ranges of dynamic detection largely limited the performances of these electrodes for BPA sensing. In recent years, the use of peptides, as sensing probes for constructing an electrochemical biosensor, has received great attention due to the following several merits: (1) peptide moieties recognize their target analytes in a

* Corresponding authors. Tel.: +82 31 290 7248; fax: +82 31 290 7272.
E-mail addresses: checws@skku.edu (W.-S. Choe), yklee@skku.edu (Y. Lee).

http://dx.doi.org/10.1016/j.bios.2014.04.009
0956-5663/© 2014 Elsevier B.V. All rights reserved.

specific manner to mimic a hormone–receptor interaction; (2) compared with other biomolecules, peptides are small and easy to synthesize in a cost-efficient manner; (3) unlike other biomolecules, the target recognition by a peptide is rarely compromised despite the structural changes in the probe molecules often encountered during the electrode fabrication. Although various peptide sequences exhibiting affinity to particular substrates have been found (Sarikaya et al., 2003), peptide molecules capable of recognizing low molecular weight organic compounds, such as BPA, have rarely been reported.

In the present study, we first screened a BPA-specific peptide sequence in order to develop a peptide-based electrochemical biosensor for BPA detection. Multiple rounds of biopanning were conducted using a combinatorial constrained peptide library displayed on an M13 phage surface and a cysteine-flanked heptapeptide sequence Cys-Lys-Ser-Leu-Glu-Asn-Ser-Tyr-Cys (CKSLENSYC) exhibiting selective affinity toward the BPA identified. The presence of two thiol groups in the screened peptide was conducive to providing a stable adhesion of peptide molecules onto the gold electrode via Au–S bonding, obviating the use of any linking agents. The formation of a self-assembled monolayer (SAM) of BPA-specific peptide molecules atop the electrode was confirmed by attenuated total reflection infrared spectroscopy (ATR-IR), cyclic voltammetry (CV) and electrochemical impedance spectroscopy (EIS). The peptide-modified gold electrode was found to directly capture BPA in the solution, and a time period of less than 5 min was sufficient before reaching the equilibrium binding. The resulting electrochemical changes monitored by differential pulse voltammetry (DPV) were proportional to the BPA concentrations; it provided a highly sensitive BPA detection in a broad range of 1–5000 nM with negligible cross reactivity to other phenolic compounds and inorganic metal ions.

2. Experiment

2.1. Materials and apparatus

BPA-1 peptide (CKSLENSYC) capable of selectively recognizing BPA was custom synthesized by Bio-FD&C (Incheon, Republic of Korea). BPA, MES hydrate, $K_4[Fe(CN)_6]$, $K_3[Fe(CN)_6]$, KCl, Tween-20, NaCl, Tris (hydroxymethyl)aminomethane (Tris), 2-nitrophenol (NP), 2,4-dinitrophenol (DNP), hydroquinone (HQ), 4-chlorophenol (CP) and phenol were purchased from Sigma Co. (USA). 4,4′-dihydroxybiphenyl (DHB) and 4,4′-(hexafluoroisopropylidene)diphenol (also known as Bisphenol AF (BPAF)) were obtained from Alfa Aesar (Great Britain). All the chemicals were used as received. HPLC-grade water (J.T. Baker, USA) was used to prepare the solutions used in this study.

Unless otherwise mentioned, all the electrochemical measurements were conducted on a VSP potentiostat (Princeton Applied Research, Oak Ridge, USA) at room temperature using a three-electrode cell comprising of a peptide-modified gold disk (CH Instruments Inc.,USA), a platinum and an Ag/AgCl (saturated KCl solution) plate as the working, counter and reference electrode, respectively. CV was conducted from −0.3 to 0.6 V at a scan rate of 50 mV s^{-1}. DPV was carried out at a sweep rate of 20 mV s^{-1} from 0 to 0.4 V and with a pulse amplitude, width and period of 2.5 mV, 50 ms and 50 ms, respectively. For electrochemical impedance spectroscopy (EIS) measurement, a sine wave of 10 mV amplitude was applied in a wide frequency range from 100 mHz to 10 kHz to the working electrode immersed in 0.1 M KCl solution containing 5 mM $[Fe(CN)_6]^{3/4-}$. EIS data were fitted to a modified mixed control circuit (Lee et al., 2008) consisting of a constant phase element (CPE), a solution resistance (Rs), an electron transfer resistance (Ret) and a Warburg impedance (W) using ZSimpWin® software (Perkin-Elmer).

Biopanning and phage binding assay were used for the screening of peptide with selective affinity toward BPA. The detailed information on the process and the result was suggested in Supplementary information.

2.2. Fabrication of the peptide-modified electrode

A gold disk electrode (2 mm in diameter) was polished and cleaned according to the literature (Lin et al., 2011b). A peptide-modified gold (peptide/Au) electrode was prepared by immersing the activated Au electrode in 0.1 M MES buffer (pH 6.8) containing 1 mg/ml of BPA-1 peptide at 4 °C overnight in order to render the formation of a self-assembled peptide monolayer atop the electrode. The peptide/Au electrode thus prepared was rinsed and stored in Tris buffer (50 mM Tris–HCl, 150 mM NaCl, 0.1% Tween-20, pH 8.0) at room temperature before use. The assembly of the peptide monolayer on the electrode surface was verified by an attenuated total reflection infrared spectroscopy (ATR-IR, Tensor 27, Bruker, Germany) analysis conducted at a resolution of 4 cm^{-1} with 50 scans. Scheme S1 (See Supplementary Information) showed the schematic drawing of the peptide modified BPA sensor.

2.3. Optimization of BPA detection condition

The peptide/Au electrode was incubated in 1 mL of Tris buffer containing 500 nM of BPA for different time periods (1, 5, 10 and 15 min). After rinsing with Tris buffer, the current response of the BPA-loaded electrode was recorded by DPV in 0.1 M KCl aqueous solution containing 5 mM $[Fe(CN)_6]^{3-/4-}$. In order to explore the effect of pH on the BPA detection, DPV responses of the peptide/Au electrode was investigated within a pH range of 5.5 to 8.5 in the presence of 500 nM BPA in Tris buffer.

2.4. Performance of the peptide/Au electrode on BPA detection

BPA powder was dissolved in 5 mL of ethanol, and the volume was adjusted to 10 mL using Tris buffer in order to give a 10 mM BPA stock solution. The standard solutions with varying concentrations of BPA were prepared by diluting the stock solution with Tris buffer. Following a 5 min incubation of the peptide/Au electrode in each BPA standard solution, the electrode was rinsed with Tris buffer in order to measure the electrochemical response of the BPA-loaded electrode by DPV in the 0.1 M KCl aqueous solution containing 5 mM $[Fe(CN)6]^{3-/4-}$. The amount of BPA captured on the peptide/Au electrode was determined by averaging the changes in the DPV peak currents from three independent measurements.

Following the electrochemical detection of BPA, the used electrode was regenerated by undergoing multiple rounds of the DPV sweep from 0 to 0.85 V in Tris buffer in order to electrochemically oxidize the captured BPA (Tu et al., 2009). Successful regeneration was confirmed by a DPV peak current change indicative of a complete dissociation of the oxidized BPA from the electrode surface.

The performance of the peptide/Au electrode in view of selective BPA detection was also investigated. For this, the electrode was incubated in Tris buffer containing 10 μM of various ionic and phenolic compounds (Ca^{2+}, Fe^{3+}, Ni^{2+}, Cu^{2+}, Zn^{2+}, SO_4^{2-}, CH_3COO^-, Fe^{2+}, phenol, DNP, NP, HQ, CP, BPAF and DHB) that are likely to co-exist with BPA and hence, interfere with the determination of BPA by exhibiting a cross binding reactivity toward the peptide probe. The extent of the cross reactivity of each interferent was assessed by comparing the DPV peak current signals recorded from the individual interferents relative to a DPV peak current signal from 100 nM BPA.

In order to demonstrate the practical applicability of the developed BPA sensor to the actual samples contaminated with BPA, mock samples containing BPA extracted from plastic products (PC pellet, PVC film, CD disc) were prepared. The extraction of BPA was conducted following the protocol reported elsewhere (Gao et al., 2012; Yu et al., 2011) but with a minor modification. Briefly, 2.0 g of each plastic product was suspended in 50 mL of distilled water, incubated with stirring at 70 °C for 48 h and subjected to filter clarification. The filtrate containing the extracted BPA was used as a mock sample with appropriate dilution.

3. Result and discussion

3.1. Fabrication of peptide/Au electrode based BPA sensor

In the electrochemical determination of BPA using gold electrodes, the dimerization of BPA due to the electrochemical oxidation of the phenolic hydroxyl group can be frequently encountered (Perez et al., 1998). This accounts for the decrease in the oxidation current often incurred with electrode poisoning, thereby rendering the necessary passivation of the electrode surface. The formation of the self-assembled monolayer (SAM) atop the electrode offers a simple and effective platform to tune the surface property for an enhanced recognition of various analytes; hence, it has been widely used for the surface passivation of electroanalytical sensors (Chen et al., 2011; Mandler and Turyan, 1996). In this aspect, the use of BPA-1 peptide as a sensing probe provides an additional merit in view of facilitating a peptide-mediated SAM formation, thereby achieving an efficient passivation of the gold electrode surface without requiring any extra linking agents and/or tedious modification/pretreatment procedures. Because the two thiol groups available in the cysteine residues flanking the heptapeptide region of BPA-1 at both ends are conducive to a spontaneous Au–S bonding between the peptide molecules and the Au surface, the assembly of a peptide monolayer atop the electrode was expedited.

The successful formation of a peptide layer on the gold electrode was confirmed by ATR-IR, as shown in Fig. 1A. The absorption peaks located at 2923 and 2852 cm^{-1} corresponded to the C–H stretching vibration of CH_3 and CH_2 in the peptide residues. The presence of Amide I band, attributed to the C═O stretching vibration of the peptide backbone, and Amide II band, assigned to the coupling of the N–H in-plane bending and C–N stretching vibration of the peptide backbone, was evidenced by the peaks at 1658 and 1546 cm^{-1}, respectively, demonstrating good agreement with those reported elsewhere (Liu et al., 2009; Zeng et al., 2014). The peaks located at 3305.8 and 1458.6 cm^{-1} were attributed to the stretching and in-plane bending vibration of O–H in –the COOH groups; C–O (Ar–OH in tyrosine) and C–N (C–NH_2 in lysine) stretching vibrations were located at 1258 and 1158 cm^{-1}, respectively.

Cyclic voltammetry (CV) was next conducted in order to probe changes in the electrochemical status of the gold surface during the electrode modification procedure. The electrochemical behavior of bare and peptide-modified gold (peptide/Au) electrodes measured by CV in 0.1 M KCl aqueous solution containing 5 mM $[Fe(CN)_6]^{3-/4-}$ at a scan rate of 50 mV/s was presented in Fig. 1B.

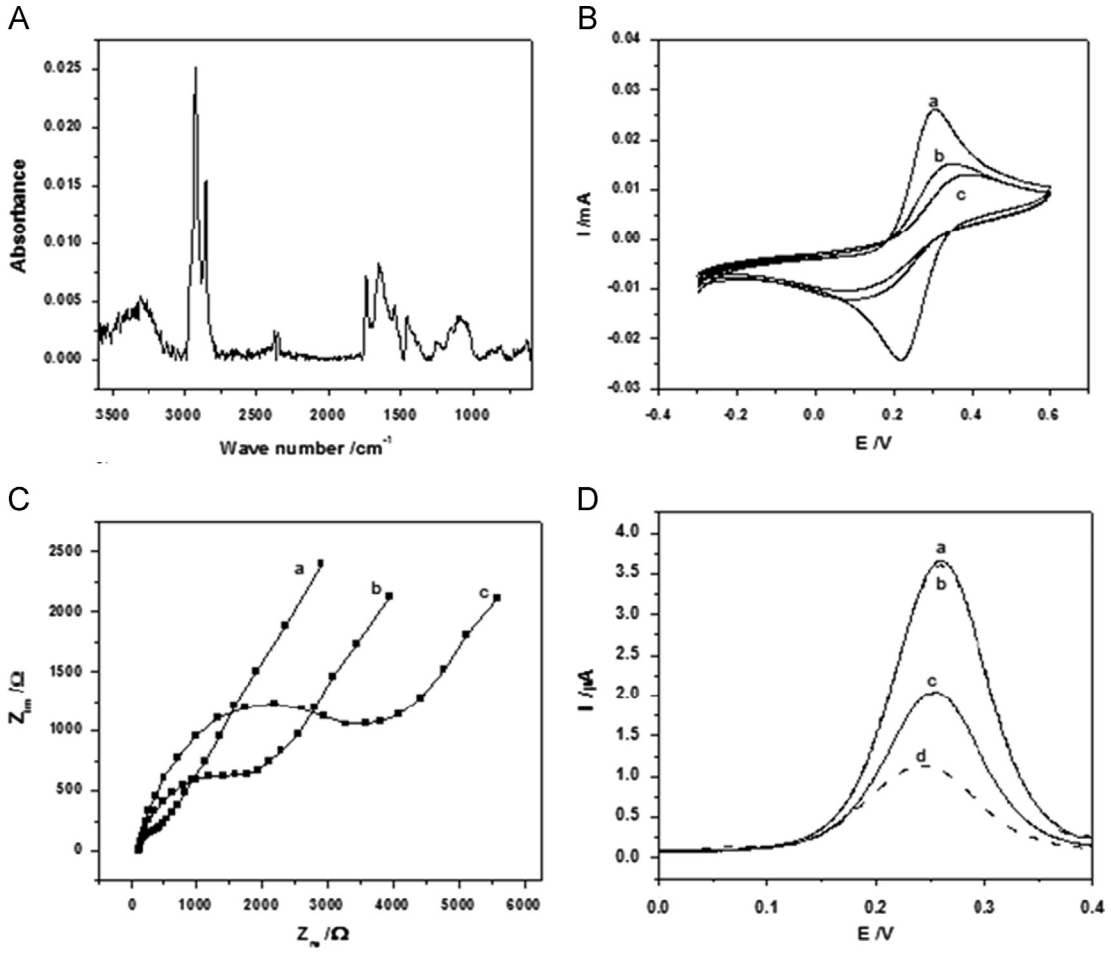

Fig. 1. Electrochemical analysis of the gold and peptide/Au electrodes fabricated in the present study. ATR-IR spectrum (A) for peptide/Au electrode. Cyclic voltammograms (B) and Nyquist plots (C) for bare Au (a), peptide/Au (b), and BPA/peptide/Au (c) electrodes. Differential pulse voltammograms (D) obtained from bare Au (a and b) and peptide/Au (c and d) electrodes incubated in 0.1 M KCl solution containing 5 mM $[Fe(CN)_6]^{3-/4-}$ in the absence (solid lines) or presence (dashed lines) of 500 nM of BPA.

A reversible CV curve with a peak to peak separation (ΔE_p) of 88 mV was observed for a bare gold electrode (curve a). In contrast, a significant decrease in the redox peak current, presumably due to the formation of an insulating peptide layer, was observed for a peptide/Au and BPA/peptide/Au electrode (curve b and c). Peptide adhesion and hence, the resulting slow electron transfer on the peptide/Au electrode, was further supported by the $\Delta E_{p,}$ which increased to 224 mV (Gao et al., 2011). After this peptide modified electrode incubated in 500 nM BPA solution, the peak current further decreased and ΔE_p increased to 293 mV, which could be attributed to the nonconductive BPA bound on the modified electrode worked with the peptide as an insulating layer to inhibit electron transfer and hamper the redox probe of $[Fe(CN)_6]^{3-/4-}$ close to the electrode surface. This result also indicated the peptide used had an excellent affinity to BPA.

In order to investigate whether the peptide layer affected the interfacial property of the bare gold electrode, electrochemical impedance spectroscopy (EIS) was conducted. The EIS spectra for bare gold, peptide/Au and BPA peptide/Au electrodes were presented in Nyquist plots (Fig. 1C), where a semicircle in the high frequency region representative of an electron transfer limited process and a straight line in the low frequency region associated with a diffusion controlled process could be visualized distinctively (Song et al., 2010; Gao et al., 2011). The bare gold electrode conveyed a very small or negligible semicircle (curve a) in the high frequency region with a calculated electron transfer resistance (R_{et}) value of 154 Ω. In contrast, the Nyquist plot for peptide/Au and BPA/peptide/Au electrode exhibited a much larger semicircle (curve b and c) with an increased R_{et} value of 2101 and 3170 Ω, indicative of a successful passivation of the electrode surface by peptide molecules and hence, the restricted access of the electrolyte (i.e., $[Fe(CN)_6]^{3-/4-}$) to the gold surface through the interfacial peptide barrier. The EIS data was in agreement with CV data, which demonstrated the peptide was successfully immobilized on the Au surface through S–Au bond and the peptide can capture the BPA with high affinity.

3.2. Electrochemical response of peptide/Au electrode upon BPA capture

The electrochemical behavior of bare gold and peptide/Au electrodes upon BPA capture was studied using differential pulse voltammetry (DPV) at the condition detailed in Section 2.1. As shown in Fig. 1D, the DPV curves and the peak oxidation current values for the bare gold electrode were almost indistinguishable before (curve a) and after (curve b) the BPA capture, indicating that the Au surface per se has no intrinsic interaction with BPA. The lack of affinity between the Au surface and BPA also provides the following important advantage: a blocking procedure often indispensable with conventional biosensors to suppress background noise signals is not strictly required for our BPA sensing platform based on the peptide/Au electrode.

The efficacy of BPA-1 peptide as an effective BPA capture probe was demonstrated by comparing the DPV responses observed for the peptide/Au electrodes (curves c and d in Fig. 1D) in the absence and/or presence of BPA. Following a 5-min incubation of the peptide/Au electrode in 500 nM BPA solution, the DPV response for the BPA-loaded electrode (curve d) showed an apparent downshift, accompanied with a significant decrease in the peak current value, clearly departing from that for the BPA-unloaded control electrode (curve c). This BPA-dependent differential DPV response of the peptide/Au electrode, in conjunction with the aforementioned DPV response of the bare gold electrode against BPA, indicates that the peptide probe solely mediated the BPA capture by the electrode. It is also noted that the DPV curve shift (i.e., from curve a to curve c) is in good agreement with the CV and EIS data, providing further evidence for the formation of an insulating peptide layer atop the gold electrode.

3.3. Optimization of sensing condition

In order to maximize the performance of peptide/Au electrodes on BPA detection, the effects of some critical factors (i.e., detection time and pH condition) on probe-target recognition were assessed. The kinetics of BPA capture by the probe peptide was investigated by monitoring the decrease in the DPV peak current values during the incubation of the peptide/Au electrode in Tris buffer containing 500 nM of BPA. The time course of the DPV peak current change (ΔI) proportional to the amount of BPA captured by the peptide/Au electrode (Fig. 2A) was found to follow the first-order kinetics, expressed as: $\Delta I = \Delta I_{max}(1 - e^{-t/\tau})$, where t is the incubation time ($_{min}$), ΔI_{max} the maximum DPV peak current change (μA), and τ is the time constant ($_{min}$), respectively. The time constant representative of the response speed of a system (i.e., the DPV peak current change mediated by peptide/Au electrode captured BPA) was estimated to be 1.48 min by a nonlinear regression, indicating that 5 min is more than sufficient to achieve an equilibrium adsorption of BPA onto the electrode at a given condition.

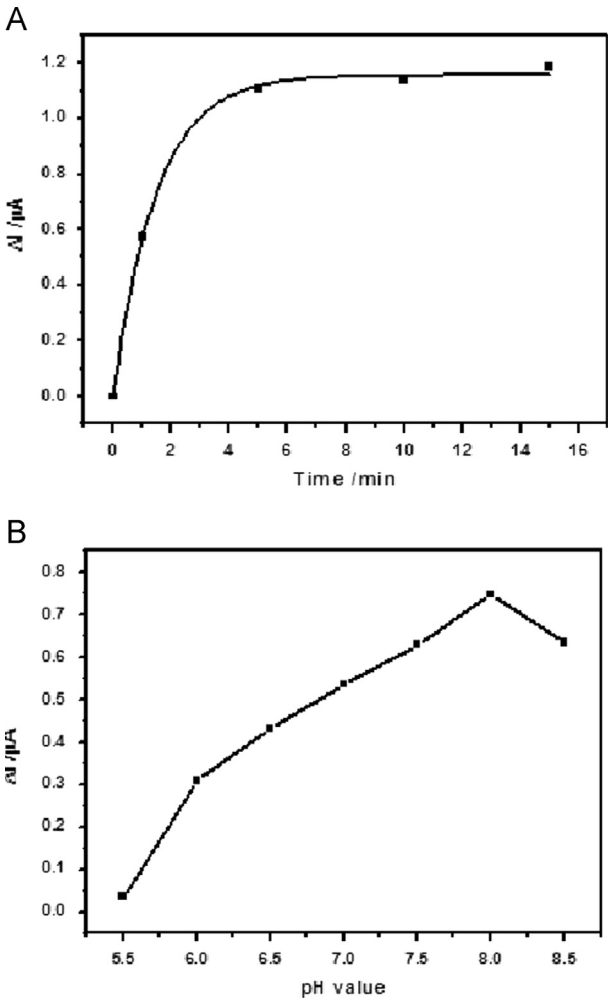

Fig. 2. The effects of incubation time (A) and pH (B) on the DPV peak current change (ΔI) of the peptide/Au electrode subjected to incubation with 500 nM of BPA. The solid line through the data in panel (A) represents the fit to the first-order kinetics model: $\Delta I = \Delta I_{max}(1 - e^{-t/\tau})$. The DPV peak current change (ΔI_{max}) and the time constant (τ) are estimated to be 1.16 μA and 1.48 min, respectively, using the χ^2 minimization procedure of OriginPro software version 8.0.

The effect of pH on the electrochemical response of peptide/Au electrode upon BPA capture was also studied by DPV. The DPV peak current change (ΔI) for each electrode following the 5-min incubation with 500 nM of BPA at varying pH conditions was found to be pH dependent, giving rise to the largest DPV peak current change (ΔI_{max}) at pH 8.0 (Fig. 2B). This indicates that the efficacy of BPA capture by the electrode is clearly affected by the solution pH at the time of probe-BPA interaction. Because the pK_a value of the phenol is 9.73 (Fernández et al., 2006), BPA is more likely to be found in a protonated and hence uncharged form in the pH range explored (i.e., 5.5–8.5). BPA-1 peptide that is used as a probe is predicted to have a pI value of 6.13 and net charges close to zero at all the pH conditions tested (the calculation is conducted by submitting the corresponding peptide sequence to the PROTEIN CALCULATOR v3.3 (http://www.scripps.edu/~cdputnam/protcalc.html)). It is therefore reckoned that an electrostatic interaction often subject to pH modulation could hardly account for the observed pH dependency of BPA recognition by the probe peptide. We are currently unable to extract any plausible clues to resolve a mechanism underpinning the pH dependent interaction between BPA and the probe peptide, which may require an in-depth understanding of their molecular recognition at an atomic level as well as an acquisition of comprehensive experimental data. Nevertheless, it was found that a five-min incubation at pH 8 would be sufficient for an efficient detection of BPA by the fabricated peptide/Au electrode; hence, all the DPV analysis pertaining to the BPA detection was conducted at this condition.

3.4. Assessment of BPA sensor performance

The performance of peptide/Au electrode-based BPA sensor was evaluated in view of the dynamic detection range, signal consistency, selectivity, spike recovery and regenerability. The amount of BPA in the solution can be quantified by monitoring an electrochemical signal, whose change is proportional to the extent of the target–probe interaction. Because the peptide/Au electrode was demonstrated to exhibit a distinctive DPV peak current change (ΔI) mediated by a specific interaction between the BPA and the affinity peptide probe immobilized on the electrode surface (Fig. 1D), a dynamic detection range of the developed sensor in BPA sensing was explored by the DPV analysis following the incubation of the electrode in Tris buffer containing varying concentrations of BPA. As shown in Fig. 3A, our sensor exhibited well-resolved DPV curves that are clearly distinguishable according to the amount of BPA captured onto the peptide/Au electrode. It was found that ΔI showed a good linear relationship to the logarithmic concentration of BPA in a broad range of 1–5000 nM with a detection limit of 0.7 nM (Thosmpson and Ellison, 2002) and an R^2 value close to 0.99 (Fig. 3A (inset)). The standard curve shown in Fig. 3A (inset) was constructed by averaging the data obtained from three peptide/Au electrodes fabricated from three independent batches. This indicates that the acquisition of very reproducible sensor signals is enabled by a lot-to-lot consistency of the sensor fabrication process. With further increase in the BPA concentration to 10 μM, the DPV curve began to level off (data not shown), presumably due to either a saturation of the binding sites afforded by the probe molecules or by the formation of insulating layers of BPA-peptide complex that are too thick at a given condition. For comparison purposes, the major performances of several BPA sensors reported elsewhere are summarized in Table 1.

Because BPA is found in diverse matrices, including wastewater, sewage and plastic extracts, it is important to evaluate how specifically the developed sensor can detect BPA for its practical implementation. In order to assess the sensor performance in view of the selective recognition of BPA, various phenolic compounds

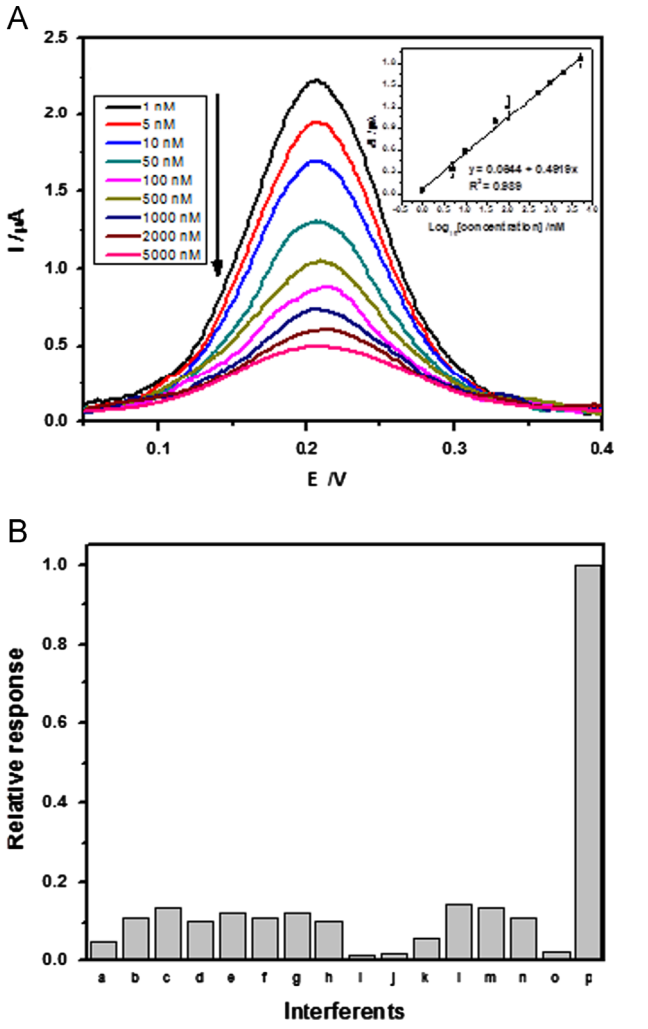

Fig. 3. Assessment of the performance of the peptide/Au electrode on detection of BPA at varying concentrations. (A) DPV response curve profiles where the peak current values decrease with BPA concentration from 1 to 5000 nM. The inset is a calibration curve from a linear relationship between the change in DPV current and logarithmic concentration of BPA (error bars represent the relative standard deviation detected for 3 times). (B) Normalized DPV peak current changes measured for the peptide/Au electrodes following their incubation with 10 μM of Ca^{2+} (a), Fe^{3+} (b), Ni^{2+} (c), Cu^{2+} (d), Zn^{2+} (e), SO_4^{2-} (f), CH_3COO^- (g), Fe^{2+} (h), phenol (i), DNP (j), NP (k), HQ (l), CP (m), BPAF (n) and DHB (o), respectively. The basis for normalization was the DPV peak current change observed for 100 nM of BPA (p).

exhibiting structural similarities to BPA were selected as representative BPA analogs capable of exhibiting cross-reactivity to the BPA affinity peptide probe. In addition, several ionic species likely to be found in the samples containing BPA were also selected as potential interferents to the BPA detection. As summarized in Fig. 3B, where DPV peak current changes (ΔI), observed for 10 μM of the above-listed BPA analogs, and interfering species were presented following the normalization against that for 100 nM of BPA, the peptide/Au electrode showed a preferential high affinity to BPA with negligible cross-reactivity to Ca^{2+}, phenol, DNP, NP and DHB. Even though the relative ΔI responses produced from the remaining BPA analogs and ionic interfering species are around 10–18% of the ΔI exhibited by BPA, considering the 100-fold higher concentration (i.e., 10 μM) of BPA analogs/interferents used for the measurement, this result is still able to demonstrate that the developed sensor is highly selective in interacting with BPA.

In order to further address the possible interference with BPA detection by unknown substances, extracts from plastic products

(e.g., PC plastic, PVC package and CD disk) were prepared to provide mock samples comprising of BPA and other unknown compounds. The extent of the interference by unknown substances on the electrochemical determination of BPA by the peptide/Au electrode was assessed by comparing DPV peak signal changes from these samples before or after the spiking of a predetermined amount of BPA (1 μM). From Table 2, spike recoveries of BPA from these mock samples were found to be 92–107%, with relative standard deviations (RSD) less than 4.4% for three independent measurements. This result suggests that the developed BPA sensor is likely to be compatible with the actual samples crowed with many undefined substances, thereby conducive to practical implementation.

The performance of the electrochemical sensor was also evaluated following regeneration of the used peptide/Au electrode by applying multiple rounds of DPV sweep, as described in Section 2.4. Upon detection of 500 nM of BPA in Tris buffer with a fresh peptide modified electrode, the same electrode was subjected to the regeneration procedure (in Fig. 4). As a result, the regenerated electrode retained its reactivity to BPA, giving rise to a reproducible DPV peak current reading indistinguishable from that of the fresh electrode. This regeneration was repeated two times before the sensor re-used. The response current remained at 80.2% of its initial peak current. The reproducibility was measured from the response to 500 nM BPA at five independent electrodes prepared under same condition. According to the result, this peptide modified electrode had a satisfied reproducibility with a RSD of 7.6%. In addition to confirmation of the reproducible BPA detection of the regenerated peptide sensor, the stability of the sensor was also studied by testing DPV responses from the sensor upon BPA detection over 30 days of storage at 4 °C. No obvious change in DPV responses was found over one month (data not shown). These results indicate that our electrochemical sensor can be used for BPA detection in a stable and reproducible manner without compromising its BPA sensing ability.

Table 1
Comparison of BPA sensing performance of the peptide/Au electrode with those reported elsewhere.

Electrode	Electrochemical Method	Linear detection range (nM)	Detection limit (nM)	Reference
PAMAM–Fe_3O_4/GCE[b]	CA[a]	10–3070	5	Yin et al. (2011)
CS– Fe_3O_4/GCE[c]	DPV	50–30000	8	Yu et al. (2011)
PAb/nano-polyTCAA[d]	EIS	4.3–430	1.3	Rahman et al. (2007)
PAb/PVC-COOH[f]	CP[e]	4.3–130	2.6	Piao et al. (2008)
tyrosinase-modified NiNP[g]	CA[b]	91–48000	7.1	Wu et al. (2012)
peptide/Au	DPV	1–5000	0.7	Our work

[a] CA: chronoamperometry.
[b] Poly(amidoamine) and iron oxide nanoparticles modified glassy carbon electrode.
[c] Chitosan-iron oxide nanocomposite modified glassy carbon electrode.
[d] Polyclonal antibody/poly(5,2′:5′2″-terthiophene-3′-carboxylic acid) modified glassy carbon electrode.
[e] Polyclonal antibody-carboxylated poly(vinyl chloride) modified carbon rod electrode.
[f] CP: chronopotentiometry.
[g] Tyrosinase-nickel nanoparticles modified screen-printed electrode.

4. Conclusion

In this study, a cysteine-flanked heptapeptide sequence (CKSLENSYC, BPA-1) exhibiting a specific affinity to bisphenol A (BPA) was identified through the biopanning procedure. By harnessing a spontaneous Au-S bonding between peptide molecules and Au surface, a novel electrochemical BPA sensor comprising of the BPA-1 peptide as a detection probe and the gold electrode as a signal transducer was successfully fabricated. The performance of the developed BPA sensor was found to be optimum at pH 8.0 for detecting BPA in less than 5 min in a wide linear dynamic detection ranging from 1 to 5000 nM. Furthermore, our BPA sensor showed superior selectivity and regeneration capability toward BPA. With all these merits, the BPA sensor developed herein is expected to find its practical application in diverse sample matrices from which fast, selective and sensitive detection of BPA is of primary concern.

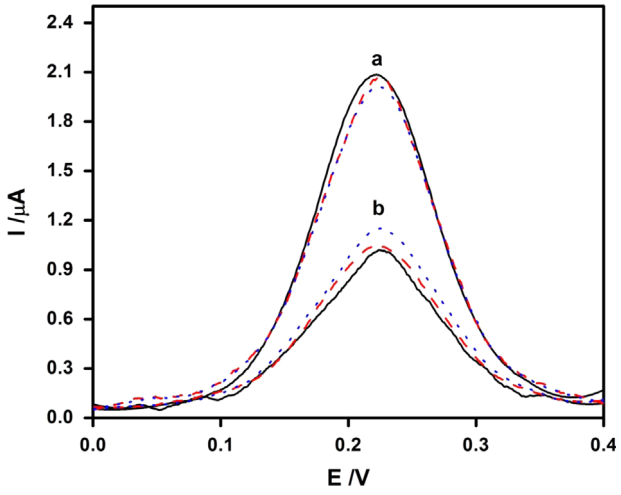

Fig. 4. Assessment of the sensor performance on BPA detection following regeneration. DPV response of peptide/Au (a) and BPA/peptide/Au (b): solid; the first sensing, dot; the first regeneration, dash; the second regeneration.

Table 2
Spike recoveries of BPA from mock samples containing BPA and other undefined substances extracted from plastic products.

Sample	BPA before spiking[a] (μM)	BPA spiked (μM)	BPA after spiking[b] (μM)	RSD[c] (%)	Spike recovery[d] (%)
CD[e]	0.89 ± 0.039	1	1.81 ± 0.1	4.37	92
PC pellet[f]	2.07 ± 0.086	1	3.14 ± 0.15	4.14	107
PVC film[g]	0.47 ± 0.015	1	1.52 ± 0.093	3.19	105

[a] The average value (three measurements) measured by as-prepared sensor.
[b] The average value (three measurements) measured by as-prepared sensor after spiking 1 μM of BPA into each mock sample.
[c] RSD: relative standard deviation for three independent measurements.
[d] Recovery = (BPA after spiking − BPA before spiking)/(BPA spiked) × 100.
[e] CD: commercial compact disc made of PC.
[f] PC: polycarbonate pellet as raw materials for fabrication of transparent PC bottle.
[g] PVC: commercial PVC films for food package.

Acknowledgment

This work was supported by Ministry of Science, ICT & Future Planning of Korea (Grant no. 2012-002285) and Basic Science Research Program through the National Research Foundation of Korea Grant funded by the Ministry of Science, ICT & Future Planning (2009-0083540).

Appendix A. Supporting information

Supplementary data associated with this article can be found in the online version at http://dx.doi.org/10.1016/j.bios.2014.04.009.

References

Chen, T., Dai, P.X., Wu, J.Y., Wang, D., Wan, L.J., 2011. J. Phys. Chem. C 115, 16583–16589.
Fan, H., Li, Y., Wu, D., Ma, H., Mao, K., Fan, D., Du, B., Li, H., Wei, Q., 2012. Anal. Chim. Acta 711, 24–28.
Fernández, L., Borrás, C., Carrero, H., 2006. Electrochim. Acta 52, 872–884.
Gao, X., Zhang, Y., Chen, H., Chen, Z., Lin, X., 2011. Anal. Biochem. 414, 70–76.
Gao, Y., Cao, Y., Yang, D., Luo, X., Tang, Y., Li, H., 2012. J. Hazard. Mater. 199–200, 111–118.
Kang, B., Kim, J.H., Kim, S., Yoo, K.H., 2011. Appl. Phys. Lett. 98 (073703), 1–3.
Lee, J.A., Hwang, S., Kwak, J., Park, S.I., Lee, S.S., Lee, K.C., 2008. Sens. Actuators B: Chem. 29, 372–379.
Lin, C.Y., Fuh, M.R., Huang, S.D., 2011a. J. Sep. Sci. 34, 428–435.
Lin, M., Yang, J., Cho, M., Lee, Y., 2011b. Macromol. Res. 19, 673–678.
Liu, Y., Chu, Z., Zhang, Y., Jin, W., 2009. Electrochim. Acta 54, 7490–7494.
Lu, Y., Peterson, J.R., Gooding, J.J., Lee, N.A., 2012. Anal. Bioanal. Chem. 403, 1607–1618.
Mandler, D., Turyan, I., 1996. Electroanalysis 8, 207–213.
Martínez-Moral, M.P., Tena, M.T., 2011. J. Sep. Sci. 34, 2513–2522.
Perez, P., Pulgar, R., Olea-Serrano, F., Villalobos, M., Rivas, A., Metzler, M., Pedraza, V., Olea, N., 1998. Environ. Health Perspect. 106, 167–174.
Piao, M.H., Noh, H.B., Rahman, M.A., Won, M.S., Shim, Y.B., 2008. Electroanalysis 20, 30–37.
Podlipna, D., Cichna-Markl, M., 2007. Eur. Food. Res. Technol. 224, 629–634.
Rahman, M.A., Shiddiky, M.J.A., Park, J.S., Shim, Y.B., 2007. Biosens. Bioelectron. 22, 2464–2470.
Ren, Y., Ma, W., Ma, J., Wen, Q., Wang, J., Zhao, F., 2012. J. Colloid Interface Sci. 367, 355–361.
Sarikaya, M., Tamerler, C., Jen, A.K.Y., Schulten, K., Baneyx, F., 2003. Nat. Mater. 2, 577–585.
Song, Z., Yuan, R., Chai, Y., Wang, J., Che, X., 2010. Sens. Actuators B: Chem. 145, 817–825.
Thosmpson, M., Ellison, S.L., 2002. Pure Appl. Chem. 74, 835–855.
Tu, X., Yan, L., Luo, X., Luo, S., Xie, Q., 2009. Electroanalysis 21, 2491–2494.
Wu, L., Deng, D., Jin, J., Lu, X., Chen, J., 2012. Biosens. Bioelectron. 35, 193–199.
Yan, W., Li, Y., Zhao, L., Lin, J.M., 2009. J. Chromatogr. A 1216, 7539–7545.
Yin, H., Cui, L., Chen, Q., Shi, W., Ai, S., Zhu, L., Lu, L., 2011. Food Chem. 125, 1097–1103.
Yu, C., Gou, L., Zhou, X., Bao, N., Gu, H., 2011. Electrochim. Acta 56, 9056–9063.
Zeng, Y., Li, W., Zhang, H., Wu, X., Sun, W., Zhu, Z., Yu, Y., 2014. Anal. Methods 6, 404–409.
Zhang, J., Li, Q., Chen, M., Li, H., Xu, Z., 2011. Sens. Actuators B: Chem. 160, 784–790.